

## Van Hove features in $\text{Bi}_2\text{Sr}_2\text{CaCu}_2\text{O}_{8+\delta}$ and effective parameters for Ni impurities inferred from STM spectra

Jian-Ming Tang and Michael E. Flatté

*Department of Physics and Astronomy, University of Iowa, Iowa City, Iowa 52242-1479*

(Received 3 May 2002; published 9 August 2002)

We present a detailed quantitative comparison between theoretical calculations of the local density of states and recent experimental measurements of scanning tunneling spectra around Ni impurities in  $\text{Bi}_2\text{Sr}_2\text{CaCu}_2\text{O}_{8+\delta}$ . A double-peak structure on the hole side of the spectrum at the Ni site is identified as the spin-split Van Hove singularity in the band structure. The Ni atom induces local changes in hopping matrix elements comparable in size to the induced on-site spin-dependent potential. We find evidence from the measurements of order-parameter suppression in the vicinity of the Ni impurity. These extracted impurity parameters can be of use in quantitative calculations of macroscopic response properties, such as the ac conductivity.

DOI: 10.1103/PhysRevB.66.060504

PACS number(s): 74.25.Jb, 74.80.-g

The response of a superconductor to impurities can determine several macroscopic electromagnetic properties, such as the magnetic penetration depth and high-frequency losses.<sup>1</sup> For high-temperature superconductors it is advantageous to study the impurity problem in real space rather than in momentum space,<sup>2</sup> not only because the impurities destroy the translational invariance, but also because these doped systems are intrinsically inhomogeneous.<sup>3</sup> High-quality electronic spectra, using the technique of scanning tunneling microscopy (STM), around individual impurity atoms in superconducting  $\text{Bi}_2\text{Sr}_2\text{CaCu}_2\text{O}_{8+\delta}$  have recently become available.<sup>4,5</sup> Quantitative comparison between calculations of the local density of states (LDOS) and these STM measurements can lead to effective impurity parameters that are useful for calculating macroscopic properties.

A number of theoretical studies of the STM spectra near impurities in *d*-wave superconductors have already been carried out by various authors.<sup>2,6-12</sup> These previous studies focused on qualitative features, such as the existence of quasiparticle resonances, the spatial structure of the resonances, and the differences among systems with various pairing symmetries. Often the model for an impurity only consisted of effective potentials at the impurity site, or relied on an unrealistic band structure for the host superconductor. There are still significant quantitative disagreements between the theoretical and experimental LDOS.<sup>10-12</sup> Of the types of impurities and defects for which high-quality STM spectra are available, the Ni impurity provides a good opportunity to resolve some of these issues. Because the perturbation to the local environment caused by a Ni impurity is weak,<sup>5,13</sup> we find that with some extensions to the potential model the STM spectra can be well reproduced by our calculations. In addition to the short-ranged potentials at the impurity site, we also include the change of the hopping matrix elements from the impurity site to its nearest neighbors, and the suppression of the order parameter.

We also find an interesting interplay between the underlying band structure and the superconducting coherence peak near a Ni impurity. In the spectrum of the Ni site there is a large peak on the hole side (below the chemical potential), right outside the gap edge. We find that this peak, previously thought as the remnant of the coherence peak, is largely con-

tributed by a density-of-states peak in the underlying band structure. One special and important feature of hole doped cuprate superconductors is that a Van Hove singularity is close to the Fermi level. It has been suggested by various authors<sup>14-20</sup> that the existence of the Van Hove singularity could affect the mechanism of superconductivity, and also account for the unusual normal-state properties. Angle-resolved photoemission (ARPES) experiments on  $\text{Bi}_2\text{Sr}_2\text{CaCu}_2\text{O}_{8+\delta}$  show that a flat band exists slightly below the Fermi surface.<sup>21,22</sup> Note that quasiparticles associated with the resulting Van Hove singularity have narrow linewidths for  $T \ll T_c$  (the conditions of Ref. 5). Despite this, a density-of-states peak (aside from the coherence peaks) in the superconducting state has never been directly reported in tunneling experiments. Traces of this feature were suggested to explain the asymmetry of the coherence peaks,<sup>23,24</sup> and the sharpness of the coherence peaks. A Van Hove peak was also found to shift the energies of the midgap impurity resonances near an impurity.<sup>25</sup>

We find that the Ni impurity provides a sensitive probe of the Van Hove peak. The Van Hove singularity is likely very close to the Fermi level, therefore, in the superconducting state the Van Hove peak cannot be resolved from the coherence peak. The Ni impurity will locally suppress the coherence peak, but only weakly perturb the underlying band structure. As a result, the Van Hove peak shows up unmasked in the spectrum at the impurity site. Our calculation is based on the following tight-binding Hamiltonian:

$$\begin{aligned}
 H = & - \sum_{\langle i,j \rangle, \sigma} (t_{ij} + \delta t_{ij}) c_{i\sigma}^\dagger c_{j\sigma} \\
 & + \sum_{\langle i,j \rangle} [(\Delta_{ij} + \delta \Delta_{ij}) c_{i\uparrow}^\dagger c_{j\downarrow}^\dagger + (\Delta_{ij}^* + \delta \Delta_{ij}^*) c_{j\downarrow} c_{i\uparrow}] \\
 & + (V_0 + V_S) c_{0\uparrow}^\dagger c_{0\uparrow} + (V_0 - V_S) c_{0\downarrow}^\dagger c_{0\downarrow}, \quad (1)
 \end{aligned}$$

where *i* and *j* label sites (the impurity resides at site 0) and  $\sigma$  labels spin. The hopping matrix elements  $t_{ij}$  are taken from a one-band parametrization of the ARPES data.<sup>26</sup> The numerical values in units of meV are 148.8, -40.9, 13, 14, and -12.8 for the hopping to the first five nearest neighbors. The

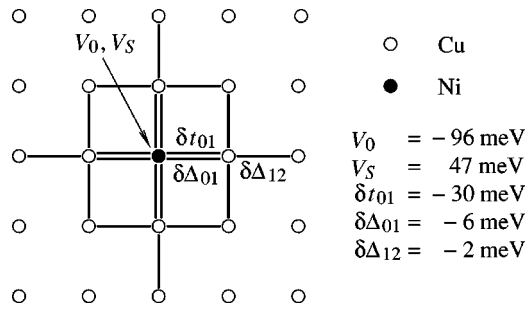


FIG. 1. A schematic diagram showing our model of a Ni impurity on the Cu-O plane. Parameters extracted from fitting to the data are listed on the right.

measured value for the gap maximum  $\Delta_0$  at a site away from the impurity is 28 meV.<sup>5</sup> The order parameters  $\Delta_{ij}$  are assumed to be real, and to have  $d$ -wave symmetry. They are only nonzero on the bonds between two nearest-neighbor sites, and  $\Delta_{i,i+\hat{x}} = -\Delta_{i,i+\hat{y}} = \Delta_0/4$ . The momentum-dependent order parameter resulting from a homogeneous system with these  $\Delta_{ij}$  is  $\Delta_{\mathbf{k}} = (\Delta_0/2)(\cos k_x - \cos k_y)$ , where the lattice spacing between two Cu atoms is unity.

We assume that the magnetism of the Ni impurity is described by a classical spin model. At the Ni site, we use a potential that consists of a magnetic part,  $V_S$ , and a nonmag-

netic part,  $V_0$ . It is found that the Ni impurity induces a change in the hopping,  $\delta t_{ij}$ , to the nearest-neighbor sites, and a suppression of the order-parameter magnitudes,  $\delta \Delta_{ij}$ , on the four bonds connected to the Ni site, and on the other twelve bonds connected to the nearest-neighbor sites. A schematic diagram of our model and the fitting parameters used for the Ni impurity are shown in Fig. 1.

Calculations presented here are based on a Koster-Slater technique.<sup>2,8,27,28</sup> The homogeneous Green's function,  $\mathbf{g}(\mathbf{r}_i, \mathbf{r}_j, \omega)$ , in the Nambu formalism is first constructed. For a given  $\mathbf{r}_i - \mathbf{r}_j$ , the computation for an energy range of 200 meV around the Fermi level with a 1-meV quasiparticle linewidth can be done in a few minutes on a personal computer. In the presence of an impurity modeled by  $\mathbf{V}$ , the Gor'kov equation,  $\mathbf{G} = \mathbf{g} + \mathbf{g}\mathbf{V}\mathbf{G} = (\mathbf{I} - \mathbf{g}\mathbf{V})^{-1}\mathbf{g}$ , is solved by numerically inverting the matrices. A single impurity only affects a few lattice sites (Fig. 1), therefore the computation for the matrix inversion can be done in less than a minute. The LDOS is the imaginary part of the Green's function,  $(-1/\pi)\text{Im}[\mathbf{G}_{11}(\mathbf{r}_i, \mathbf{r}_i, \omega) - \mathbf{G}_{22}^*(\mathbf{r}_i, \mathbf{r}_i, -\omega)]$ .

In the following, we will discuss how various parameters influence our calculations. Although six parameters including the chemical potential are introduced in the model, there are particular features in the LDOS spectra associated with each of them. This allows us to determine each parameter mostly independent from the others.

Let us first consider the chemical potential. From the ARPES parametrization,<sup>26</sup> the chemical potential for an optimally doped sample is  $-130.5$  meV. However, we know from STM measurements that the doping concentration is locally varying, and is correlated with the superconducting

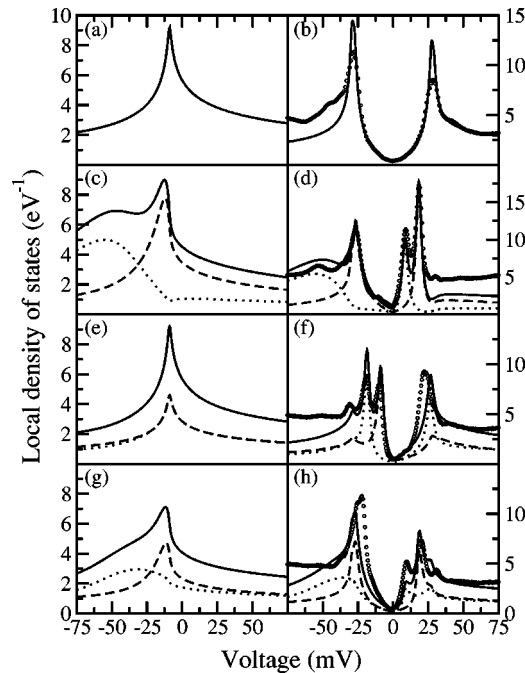


FIG. 2. LDOS spectra at various sites near a Ni impurity. The left panels show the spectra in the normal state (Ref. 30). The right panels show the spectra in the superconducting state. Solid lines show the calculated results. Dashed and dotted lines show the two spin components. (a) and (b) are the spectra at a site about 30 Å away from the Ni impurity. (c) and (d) are the spectra right at the impurity site. (e) and (f) are the spectra on the nearest-neighbor site. (g) and (h) are the spectra on the next-nearest-neighbor site. Open circles (o) show the STM data (Ref. 5). The data was rescaled by a constant factor identical for all the spectra.

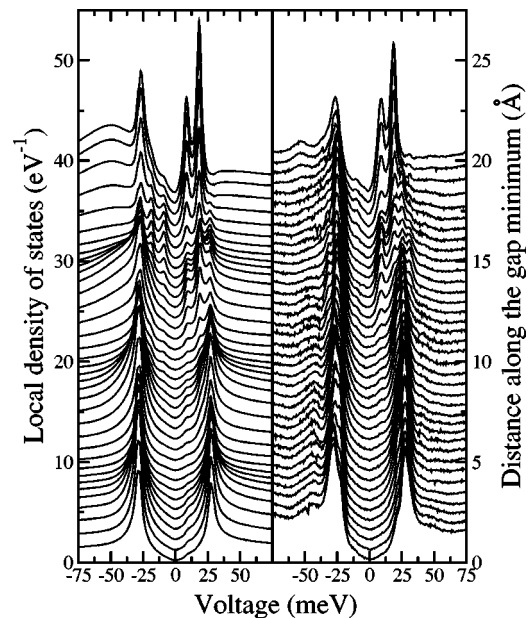


FIG. 3. Evolution of the spectra as a function of distance from the Ni atom. Left panel shows the calculations and the right panel shows the data from Fig. 4 in Ref. 5. The spin splitting of the resonance peaks inside the gap is constant as one moves away from the impurity site. The spin splitting of the Van Hove singularity decreases as the distance increases.

gap magnitude.<sup>3</sup> A region with a gap magnitude of 28 meV is overdoped. The fit to STM spectra is optimal if the shift in chemical potential relative to the optimally doped region is about  $-25$  meV. This amount of shift changes the location of the Van Hove singularity from 34 meV to 9 meV below the Fermi level, shown in Fig. 2(a) for  $\Delta_{ij}=0$ .<sup>29</sup> In the superconducting state the Van Hove singularity cannot be resolved from the coherence peak at the hole side, shown in Fig. 2(b). The chemical-potential shift also sharpens the coherence peaks and contributes to the asymmetry between the two peaks. Although not direct evidence for the Van Hove singularity in STM, the agreement between the calculations and the measurements is certainly improved.

We now describe the modeling of the Ni impurity focusing first on the single-site potential model with only the on-site potentials  $V_0$  and  $V_S$ . For a weak potential, the main effect of these potentials is to set the energies of the resonances. Since the resonance peaks for Ni are at 9.2 and 18.6 meV, and the perturbation from Ni is weak, both  $V_0 + V_S$  and  $V_0 - V_S$  should be negative. Our  $V_0$  does not differ greatly from that found in a simple model.<sup>31</sup> The two on-site parameters,  $V_0$  and  $V_S$ , are both required to fit the energies of the two resonance peaks.<sup>32</sup> Note that we have no control over the peak height or width in the spectra using this simple model. We find, due to extended states within the gap, that the resonance peaks will be broader than the coherence peaks. In the observation, however, the width of the resonance peaks appears comparable, or even sharper, than the coherence peaks.

In order to reduce the coupling to the extended states and increase the localization of the resonance states, we then as-

sume that the hopping to the nearest-neighbor sites,  $\delta t_{01}$ , is reduced. With only a 20% change in the nearest-neighbor hopping, we can reproduce the linewidth of the resonance peaks.  $V_0$  and  $V_S$  must be adjusted slightly when  $\delta t_{01}$  is introduced in order to keep the resonances at the fixed energies. Our calculations show that the magnitudes of the on-site potentials change to even weaker values, and characterize an even weaker impurity potential. Using these three parameters for calculating the effect of a Ni impurity in the normal state [shown in Fig. 2(c)], one can see that the band structure is not highly distorted. The Van Hove peak remains reasonably sharp, and splits into two spin components. Comparing Fig. 2(c) to the superconducting state shown in Fig. 2(d), we can identify the two peaks on the hole side, right outside the gap edge, as the spin-split Van Hove peaks. A similar connection between the normal-state electronic structure and an impurity's influence on the superconducting state has been identified in calculations for impurities in  $s$ -wave superconductors.<sup>27,28</sup> Another distinction between the mid-gap resonances and the Van Hove peaks is that the spin splitting of the resonance peaks inside the gap remains independent of distance from the impurity site. The spin splitting of the Van Hove singularity, however, decreases as the distance increases.

Once the large peak at the hole side was identified as the Van Hove peak, a noticeable disagreement between the calculation and the data became apparent. The calculated relative energy difference between the resonance peaks and the Van Hove peaks is somewhat larger than the observed value if the gap maximum is constant everywhere. In the  $d$ -wave superconducting state, the position of the Van Hove peak is

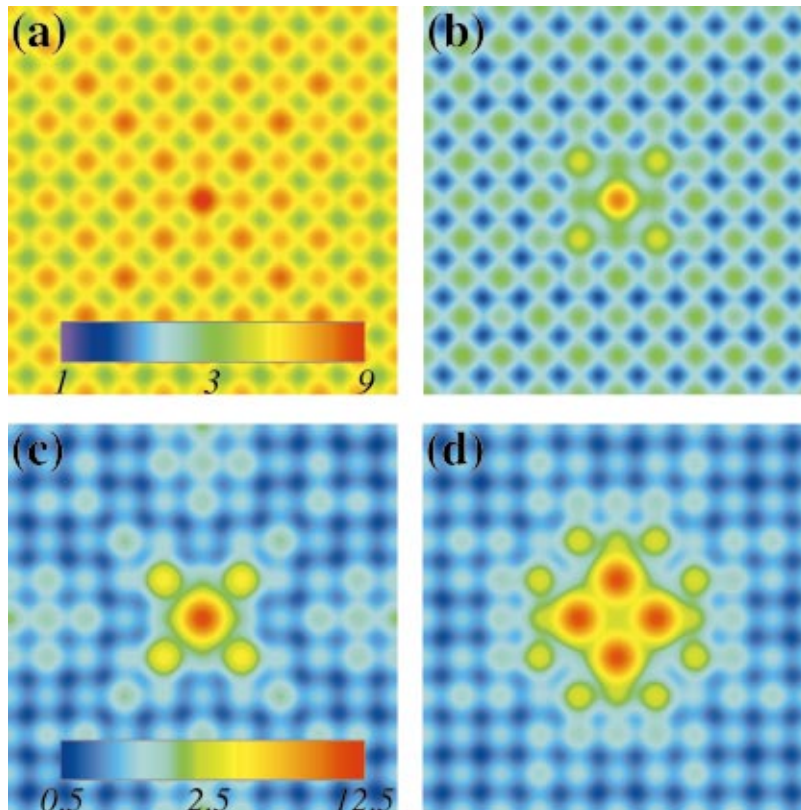


FIG. 4. (Color) Spatial structure of the LDOS around a Ni impurity in the normal state at (a)  $-15$  meV, (b)  $-50$  meV [near Van Hove peak positions in Fig. 2(c)], and in the superconducting state at (c)  $+9$  meV and (d)  $-9$  meV. The Wannier function is assumed to be Gaussian with a width of half the lattice spacing. The LDOS is shown in logarithmic scale and in units of  $\text{eV}^{-1}$ . The color bar for (b) is the same as for (a) and the color bar for (d) is the same as for (c). The lattice orientations in (c) and (d) need to be rotated by  $45^\circ$  when compared to Fig. 2 in Ref. 5.

dominated by the gap edge. One cannot increase the agreement by tuning  $V_0$  because that shifts all peaks by almost an equal amount of energy. We could obtain good agreement if the gap maximum were about 22 meV instead of 28 meV. In principle, self-consistent calculations can account for this effect, however, the self-consistency conditions involve the pairing mechanism, which is controversial. Taking a phenomenological approach, we can identify the suppression of the order parameter around the impurity from the data. This then becomes a constraint on pairing theory. We find that the parameter is locally suppressed more than 50% (see Fig. 1).

So far, we were only fitting the spectrum right at the Ni site. Nevertheless, good agreement in spatial structure is also obtained. Detailed comparisons for the spectra on neighboring sites are shown in Figs. 2(e)–(h), the spatial decay of the resonance peaks is shown in Fig. 3, and the spatial maps at given energies are shown in Fig. 4. These are direct comparisons with the data in Figs. 2–4 of Ref. 5.

Two key additional features are found from the spatial structure. The first one is that the hole component of the resonance has  $d$ -wave symmetry.<sup>2,13</sup> The second is that the perturbation, due to the Van Hove singularity, is strongest along the diagonals of the lattice. At a given energy, the secondary peaks are always located at the next-nearest-neighbor sites rather than the nearest-neighbor sites relative to the main peaks. This is because, around the Fermi level, the saddle points that give rise to the Van Hove singularity in the density of states are near the  $(\pm\pi, 0)$  and  $(0, \pm\pi)$  points in momentum space. The main contribution to the real-space Green's function largely comes from these high density-of-states regions,

$$\mathbf{g}(\mathbf{r}_i, \mathbf{r}_j, \omega) = \int \frac{d^2\mathbf{k}}{(2\pi)^2} e^{i\mathbf{k}\cdot(\mathbf{r}_i - \mathbf{r}_j)} \mathbf{g}(\mathbf{k}, \omega). \quad (2)$$

For  $\mathbf{r}_i - \mathbf{r}_j = (\pm 1, \pm 1)$ , the four regions add up constructively, while for  $(\pm 1, 0)$  or  $(0, \pm 1)$ , the contributions from  $(\pm\pi, 0)$  cancel with those from  $(0, \pm\pi)$ . As a result,  $|\mathbf{g}((1, 1), (0, 0), \omega)| \gg |\mathbf{g}((1, 0), (0, 0), \omega)|$  for energies near the chemical potential. This is also consistent with the larger spin splitting of the Van Hove peak at the next-nearest-neighbor sites compared to the nearest-neighbor sites.

In this study we have assumed that the STM spectra are directly related to the electronic structure of the Cu-O plane regardless of the presence of the intermediate Bi-O plane. As was argued in Ref. 5, the energies and linewidths of the resonances should be the same. We find the principal effect of a  $d$ -wave filter<sup>33</sup> in our parametrization is to (roughly) change the sign of  $V_0$ . Therefore, the evidence for the reduction of hopping and suppression of the order parameter are still clear.

In summary, the presence of a Ni atom on the Cu-O plane produces a weak perturbation to the system. We show direct evidence for a density-of-states peak in the STM measurements and local suppression of the order parameter. The suppression of the order parameter can constrain the self-consistency condition and thus the pairing mechanism.

We thank E. W. Hudson and J. C. Davis for providing data shown in Figs. 3 and 4 of Ref. 5. This work was supported by the ONR Grant No. N00014-99-1-0313.

- 
- <sup>1</sup>M. Tinkham, *Introduction to Superconductivity*, 2nd ed. (McGraw-Hill, New York, 1995).
- <sup>2</sup>M.E. Flatté and J.M. Byers, in *Solid State Physics*, edited by H. Ehrenreich and F. Spaepen (Academic Press, New York, 1999), Vol. 52, pp. 137–228.
- <sup>3</sup>S.H. Pan *et al.*, *Nature (London)* **413**, 282 (2001).
- <sup>4</sup>S.H. Pan *et al.*, *Nature (London)* **403**, 746 (2000).
- <sup>5</sup>E.W. Hudson *et al.*, *Nature (London)* **411**, 920 (2001).
- <sup>6</sup>J.M. Byers, M.E. Flatté, and D.J. Scalapino, *Phys. Rev. Lett.* **71**, 3363 (1993).
- <sup>7</sup>M.I. Salkola, A.V. Balatsky, and D.J. Scalapino, *Phys. Rev. Lett.* **77**, 1841 (1996).
- <sup>8</sup>M.E. Flatté and J.M. Byers, *Phys. Rev. Lett.* **80**, 4546 (1998).
- <sup>9</sup>S. Haas and K. Maki, *Phys. Rev. Lett.* **85**, 2172 (2000).
- <sup>10</sup>M.E. Flatté, *Phys. Rev. B* **61**, R14 920 (2000).
- <sup>11</sup>A. Polkovnikov, S. Sachdev, and M. Vojta, *Phys. Rev. Lett.* **86**, 296 (2001).
- <sup>12</sup>J.-X. Zhu and C.S. Ting, *Phys. Rev. B* **64**, 060501 (2001).
- <sup>13</sup>M.E. Flatté, *Nature (London)* **411**, 901 (2001).
- <sup>14</sup>J.E. Hirsch and D.J. Scalapino, *Phys. Rev. Lett.* **56**, 2732 (1986).
- <sup>15</sup>P.A. Lee and N. Read, *Phys. Rev. Lett.* **58**, 2691 (1987).
- <sup>16</sup>J. Labbé and J. Bok, *Europhys. Lett.* **3**, 1225 (1987).
- <sup>17</sup>J. Friedel, *J. Phys.: Condens. Matter* **1**, 7757 (1989).
- <sup>18</sup>R.S. Markiewicz, *J. Phys.: Condens. Matter* **2**, 665 (1990).
- <sup>19</sup>J.M. Getino, H. Rubio, and M. de Llano, *Solid State Commun.* **83**, 891 (1992).
- <sup>20</sup>D.M. Newns *et al.*, *Comments Condens. Matter Phys.* **15**, 273 (1992).
- <sup>21</sup>Z.X. Shen and D.S. Dessau, *Phys. Rep.* **253**, 1 (1995).
- <sup>22</sup>J. Ma *et al.*, *Phys. Rev. B* **51**, 3832 (1995).
- <sup>23</sup>C. Renner and Ø. Fischer, *Phys. Rev. B* **51**, 9208 (1995).
- <sup>24</sup>J. Bok and J. Bouvier, *Physica C* **274**, 1 (1997).
- <sup>25</sup>M. Crisan and I. Tifrea, *Physica B* **259-261**, 462 (1999).
- <sup>26</sup>M.R. Norman *et al.*, *Phys. Rev. B* **52**, 615 (1995).
- <sup>27</sup>M.E. Flatté and J.M. Byers, *Phys. Rev. Lett.* **78**, 3761 (1997).
- <sup>28</sup>M.E. Flatté and J.M. Byers, *Phys. Rev. B* **56**, 11 213 (1997).
- <sup>29</sup>The normal state in cuprates is known to have a variety of unusual properties. Thus the state with  $\Delta_{ij}=0$  may or may not correspond to the true normal state of the solid. We will, however, use the term “normal state” in this paper to refer to that state with the Hamiltonian of Eq. (1), but with  $\Delta_{ij}=0$ .
- <sup>30</sup>The peaks shown in Figs. 2(a), 2(c), 2(e), and 2(g) may not be visible due to the large linewidth in the true normal state.
- <sup>31</sup>R. Fehrenbacher, *Phys. Rev. Lett.* **77**, 1849 (1996).
- <sup>32</sup>M.I. Salkola, A.V. Balatsky, and J.R. Schrieffer, *Phys. Rev. B* **55**, 12 648 (1997).
- <sup>33</sup>I. Martin, A.V. Balatsky, and J. Zaanen, *Phys. Rev. Lett.* **88**, 097003 (2002).